Journal of the Energy Institute 90 (2017) 825–837

Contents lists available at ScienceDirect

Journal of the Energy Institute

journal homepage: http://www.journals.elsevier.com/journal-of-the-energy-institute

Pyrolysis kinetics of walnut shell and waste polyolefins using thermogravimetric analysis

Başak Burcu Uzun [a], Elif Yaman [b, *]

[a] Department of Chemical Engineering, Faculty of Engineering, Anadolu University, 26555 Eskişehir, Turkey
[b] Central Research Laboratory, Bilecik Şeyh Edebali University, 11210 Bilecik, Turkey

ARTICLE INFO

Article history:
Received 21 March 2016
Received in revised form
6 September 2016
Accepted 12 September 2016
Available online 21 September 2016

Keywords:
Thermogravimetry
Co-pyrolysis
Walnut shell
Kinetics
Polyolefins

ABSTRACT

Co-pyrolytic behavior and kinetics of walnut shell (WS), polypropylene (PP), low density polyethylene (LDPE) and their blends were investigated using a thermogravimetric analyzer. WS and plastic samples were blended weight proportion of 1:2; 1:1 and 2:1. The desired final temperature of 650 °C was achieved at five different heating rates (5, 10, 15, 20 and 50 °C min^{-1}). Three devolatilization stages of WS were determined as removal of water, decomposition of hemicellulose and cellulose, and lignin. On the other hand, the degradation curves of PP and LDPE showed only one stage belonging to decomposition of polyene chains. The kinetic parameters like activation energy and pre-exponential factor of pyrolysis zone were determined by applying Arrhenius and Coats Redfern method. According to Arrhenius method, the average value of activation energies of WS, PP and LDPE were 69.32, 295.65 and 254.55 kJ mol^{-1}, respectively. Moreover by using Coats Redfern method, average value of activation energies of WS, PP and LDPE were determined as 101.58, 333.53 and 316.77 kJ mol^{-1}, respectively. As the pyrolysis reaction advanced the Arrhenius parameters (E and A) increased or decreased simultaneously, exhibiting a compensation effect.

1. Introduction

Concern of climate change and the harmful impacts of acid rain encouraged the researchers for new and cleaner methods of electric power generation [21]. Burning of fossil fuels is increased CO_2, NO_x ans SO_x emissions so their environmental impact is also increasing. In addition, the increasing consumption of these non-renewable fuels gives the impression that their quantity is finite. Thus, energy from biomass could promote to decrease the consumption of fossil fuels, by means of reducing environmental and energy problems. Currently, 14% of the world's total energy needs is supplied by biomass [12]. Pyrolysis, thermolysis, gasification and combustion, as characterization studies of lignocellulosic biomass, have been carried out by many researchers in order to design efficient and environmentally sustainable processes [9,19,24,28,29,34,37,40,42]. Biomass type can significantly influence heat transfer and reaction rates, such that the optimal operating conditions are highly variable. Biomass and organic residues can convert into diverse product by pyrolysis. Its application may essentially diversify the energy-supply in many situations, leading to a more secure and sustainable global energy-supply chain [26].

The 60% of solid urban waste is plastics from containers and packaging so the plastic materials have became an important part of this type of waste. The composition of the plastic part is mainly polyolefins (high and low density polyethylene, polypropylene and polystyrene), accounting for around 70% of the total plastic waste. Plastics are mostly non-biodegradable; these strong uses have led to the generation of an increased amount of plastic waste. Different techniques have been implemented by researchers to decrease negative impact of waste plastics on the environment. Leaching and soil impregnation of plastics degradation products produce several pollutants (nitrous and sulfur oxides, dusts, dioxins and other toxins) that have a highly negative impact on the environment, so landfilling or incineration of this type of waste are not the right solutions. Recovery of the organic content of plastic waste should be part of the organic life-cycle but both processes do not allow the recovery of the organic content of plastic waste [1].

* Corresponding author.
E-mail address: elif.yaman@bilecik.edu.tr (E. Yaman).

http://dx.doi.org/10.1016/j.joei.2016.09.001
1743-9671/

The conversion of lignocellulosic and plastic waste into valuable products such as chemicals or fuels via thermal co-processing treatment methods is environmentally friendly ways. Polyolefinic polymers which contain approximately 14 wt.% hydrogen, can provide hydrogen during thermal co-processing with wood biomass. Acting as hydrogen source of polyolefines can lead to an increase of liquid production. The synergistic effects observed for co-liquefaction of biomass–plastic mixtures lead to an increase in oil yields. On the other side, biomass gives highly oxygenated pyrolysis oils because of low carbon content of 47–51 wt.% and high oxygen content of 42–46 wt.%. However, synthetic polymeric materials such as waste polyolefines have very high carbon content of about 84 wt.% and low oxygen content of about 1.5 wt.% producing hydrocarbon oils by pyrolysis.

Co-processing of synthetic polymers with biomass could balance the carbon, oxygen and hydrogen in the feedstock, with strong effects on the properties of degradation products. Biomass has lower thermal stability compared to plastics and thus it could affect their radical degradation mechanism by promoting the degradation of synthetic macromolecules. In the co-pyrolysis, the yields and composition of the products strongly depends on the treatment method, processing conditions, type of biomass and of synthetic polymers [11,49].

Kinetic analysis of thermal decomposition processes has been the subject interest for many investigators all along the modern history of thermal decomposition. The interest is fully justified. On one side, kinetic data are essential for designing any kind of device, in which the thermal decomposition takes place; on the other side, kinetics is intrinsically related with the decomposition mechanisms. The knowledge of the mechanism allows the postulation of kinetic equations or vice versa, and kinetics is the starting point to postulate mechanisms for the thermal decomposition [17]. Thermogravimetric analysis (TGA) is one of the most common techniques used to investigate thermal events and kinetics during pyrolysis of solid raw materials such as coal, biomass and plastic. It provides a measurement of weight loss of the sample as a function of time and temperature. The kinetics of these thermal events has been determined by the application of the Arrhenius equation corresponding to the separate slopes of constant mass degradation [49].

Considering the kinetics of plastic-biomass co-pyrolysis numerous recent studies on the TGA pyrolysis of plastics [1,13,27,30] and biomass [4,26,31,33,36] Uzun & Sarioglu, 2009 [50] are available and most were based on different calculations methods.

Presently, the shell of the edible nuts walnut has been selected as biomass. *Walnut* shell, an agricultural waste, is the lingo-cellulosic material forming the thin endocarp or husk of the walnut tree fruit. In 2012, walnut production was about 203,212 tonnes in Turkey [51]. 136,150 tonnes of walnut shell was left behind in 2012, since it comprises 67% of the total weight of the fruit. The walnut shell as lignocellulosic biomass is a good precursor for pyrolysis process [7,15]. In the literature walnut shell is used as a precursor for co-pyrolysis process together with coal and tar sand [23,47]. Walnut shell can be also pyrolyzed together with polyolefins. Polyolefins, which can be called as engineering plastics, has increased significantly in recent decades largely due to their low cost, good mechanical properties and light weight. On the other hand, this increase in usage has also created many challenges associated with disposal and their impact on the environment. In that, polyolefins do not easily degrade in the natural environment and hence the need for clean conversion technologies has become a major topic of research. There is no sufficient study on co-pyrolysis kinetics of walnut shell and waste polyolefins in the literature. In this study, waste polypropylene (PP) and low density polyethylene (LDPE) were selected as waste polyolefin samples. Co-pyrolytic behaviors of WS-PP and WS-LDPE blends were investigated under inert atmosphere using a thermogravimetric analyzer. Thermogravimetric analysis were carried out at five different heating rates (5, 10, 15, 20 and 50 °C min^{-1}), and the related kinetic parameter, activation energy (E), pre-exponential factor (A) were calculated by Arrhenius and Coats Redfern methods in order to evaluate *Walnut*, PP and LDPE as a potential feedstock for thermochemical conversion.

2. Experimental technique

2.1. Raw material collection and sample preparation

The feedstock materials used in this study included *Walnut shell* (WS) from Bilecik located in the north west of Turkey, as well as commercially available (MTM Recycling Company, Turkey) waste polypropylene (PP) and waste low density polyethylene (LDPE). Air-dried biomass sample was ground in a high speed rotary cutting mill and sieved to give fractions of 224 < Dp < 425 μm, 425 < Dp < 600 μm, 600 < Dp < 850 μm, 850 < Dp < 1250 μm and 1250 < Dp < 1800 μm. 425–600 μm mesh size samples were used in all experiments. Waste plastic samples were grounded cryogenically and <224 μm mesh size sample were chosen for all experiments. ASTM Standard Test Methods for proximate analysis were used to determine the weight fractions of volatile, ash and fixed carbon contents. The weight fraction of moisture content was measured in Sartorius MA 150 moisture analyzer. The ultimate analysis of Walnut shell, PP and LDPE was performed in an elemental analyzer (Leco CHN628 Series). The heating value is a substantial thermal property to design and evaluate of thermal conversion systems.

The gross calorific values were calculated by Dulong formula [22]:

$$Q_{GVC} = 338.2C + 1442.8\left(H - \frac{O}{8}\right) \quad \left(kJ\ kg^{-1}\right) \tag{1}$$

C, H, N, O and S are the mass fractions of carbon, hydrogen, nitrogen and oxygen. The main characteristic properties of *walnut* shell are given in Table 1. More detailed characteristic properties of walnut shell can be found in previous study [39]. The main characteristic properties of PP and LDPE are also given in Table 2. The FTIR spectrum of PP and LDPE which shows indications of various surface functional groups is shown in Figs. 1 and 2, respectively.

2.2. Pyrolysis

Pyrolysis experiments were carried out with a thermogravimetric analyzer (Setaram Labsysevo, France). The biomass/plastic samples were blended (1:1 weight ratio) in an agate mortar to achieve homogeneity. 100 μL Al_2O_3 crucible was used for each run, and the experiments were carried out non-isothermal conditions. 10 ± 3 mg of sample was pyrolyzed from room temperature to 650 °C at heating rates of

Table 1
Main characteristic properties of walnut shell.

Characteristics	Method	
Moisture content[a] (%)	Moisture analyzer	8.06
Holocellulose (%)	TS 4431	46.13
Oil (%)	TS 769	3.29
Lignin	[25]	48.11
Ectrastives	[25]	3.78
Hemicellulose	[25]	22.18
Cellulose	By difference	23.95
Proximate analysis[b]		
Ash (%)	ASTM D 1102-84	0.33
Volatile matter (%)	ASTM E 897-82	76.38
Fixed carbon (%)	By difference	15.21
Ultimate analysis		
Carbon (%)	Elemental analyzer	47.50
Hydrogen (%)	Elemental analyzer	6.39
Nitrogen (%)	Elemental analyzer	0.46
Oxygen (%)	By difference	45.65
Empirical formula	By calculation	$CH_{1.61}N_{0.008}O_{0.75}$
H/C molar ratio	By calculation	1.61
O/C molar ratio	By calculation	0.75
Higher calorific value (MJ/kg)	Dulong formula	16.69

[a] As received.
[b] Weight percentage on dry basis.

Table 2
The main characteristic properties of PP and LDPE.

Characteristic	Method	
Ultimate analysis		*PP*
Carbon (%)	Elemental analyzer	83.28
Hydrogen (%)	Elemental analyzer	13.61
Nitrogen (%)	Elemental analyzer	0.16
Oxygen (%)	By difference	2.96
Empirical formula	By calculation	$CH_{1.96}N_{0.002}O_{0.03}$
H/C molar ratio	By calculation	1.96
O/C molar ratio	By calculation	0.03
Higher calorific value (MJ/kg)	Dulong formula	47.26
Ultimate analysis		*LDPE*
Carbon (%)	Elemental analyzer	81.80
Hydrogen (%)	Elemental analyzer	13.52
Nitrogen (%)	Elemental analyzer	0.29
Oxygen (%)	By difference	4.39
Empirical formula	By calculation	$CH_{1.98}N_{0.003}O_{0.03}$
H/C molar ratio	By calculation	1.98
O/C molar ratio	By calculation	0.03
Higher calorific value (MJ/kg)	Dulong formula	46.38

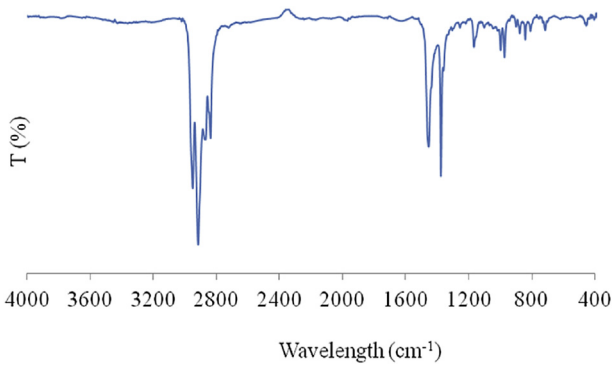

Fig. 1. FTIR spectrum of PP.

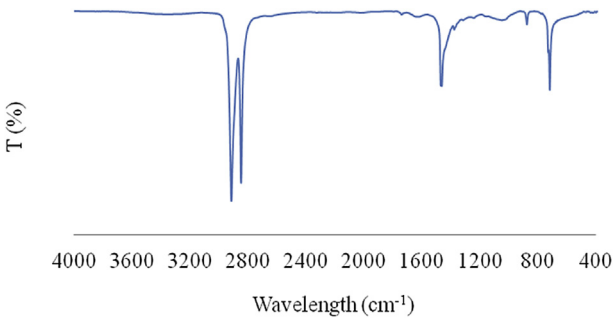

Fig. 2. FTIR spectrum of LDPE.

5, 10, 15, 20, 50 °C min^{-1}. Nitrogen was used as an inert purge gas to displace air in the pyrolysis zone, thus avoiding undesirable oxidation of the sample. After the initial purging, nitrogen was flowed 20 mL min^{-1}

3. Results and discussion

3.1. Pyrolysis of WS, PP, LDPE and their blends

The results of main characteristic properties of WS, PP and LDPE are presented in Tables 1 and 2. Higher calorific values were calculated from elemental analysis results by using Dulong's formula [22]. The higher calorific values of WS, PP and LDPE are 16.69 MJ kg^{-1}, 47.26 MJ kg^{-1} and 46.38 MJ kg^{-1} , respectively.

FTIR spectrum of PP and LDPE are given in Figs. 1 and 2. In Fig. 1, peak positions of 1458, 1375, 1167 cm^{-1} indicates that PP has aliphatic hydrocarbon with brunched chain, 2951, 2877, 1458, 1375 cm^{-1} indicates that PP has alkyl group-methyl substituent and 2951, 1458, 1375, 1167, 973 cm^{-1} indicates that PP has aliphatic hydrocarbon with highly branched chain. According to Fig. 2, LDPE has aliphatic hydrocarbon groups with long chain (2921, 2846, 1471, 1377, 729 cm^{-1}), alkyl groups-long chain compound (2921, 2846, 1464, 720 cm^{-1}) and aliphatic hydrocarbon groups-possibly long chain crystalline (2921, 1464, 729, 720 cm^{-1}).

Fig. 3 shows the thermogravimetric and derivative thermogravimetric curves of walnut shell, under inert atmosphere for the final temperature 1000 °C heating rate of 20 °C min^{-1}.

According to TG curve of WS, the mass lose range can be divided into three step because of variable-slope curves. The first step starts at 60 °C and finishes at about 140 °C. This could have been owing to the vaporization of the moisture in consequence of physically absorbed water of the sample. Following the TG curve the main devolatilization step begins at 220 °C and finishes at 394 °C. This step indicates decomposition of hemicellulose and cellulose referred as “active pyrolysis zone” since mass loss rate is high. After 415 °C “passive pyrolysis zone” started and mass loss rate is lower at this step. Then, there is no further weight loss essentially. These thermal behaviors clarified by the components of WS. WS is mainly consisted of hemicellulose, cellulose and lignin like all other lignocellulosic materials. The

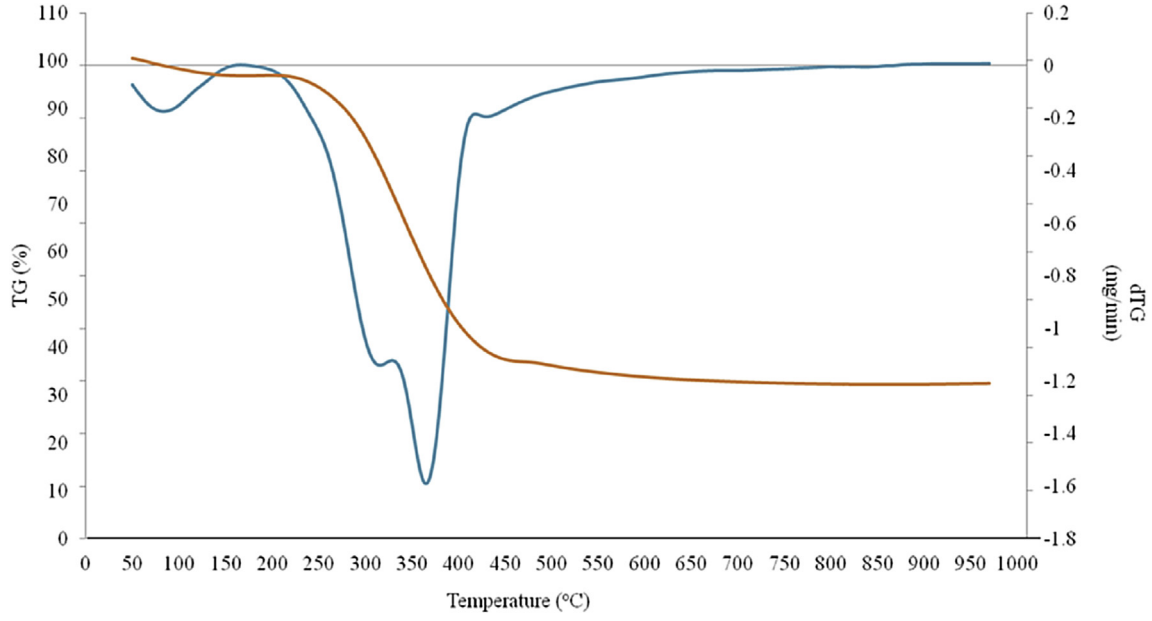

Fig. 3. The thermogravimetric curves of WS (heating rate of 20 °C min^{-1}).

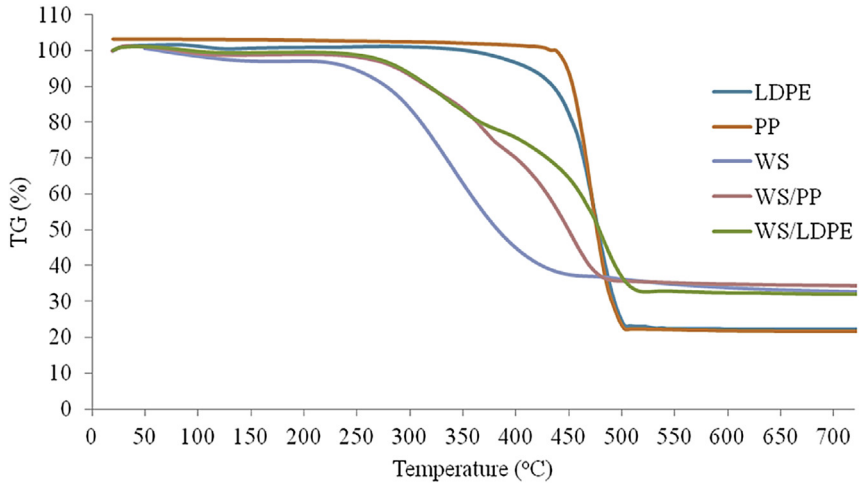

Fig. 4. TG curves of LDPE, PP, WS, WS/PP and WS/LDPE.

thermogravimetric behavior of these components have been studied before and it is well known that hemicellulose, cellulose and lignin accomplished their decomposition within the temperature ranges of 210–325, 310–400, and 160–900 °C, respectively [38]. Based on these temperature intervals, the minor and major reactions observed in active pyrolysis zone can be attributed to decomposition of hemicellulose and cellulose. From Table 1, the sum of hemicellulose and cellulose amount is calculated as 46.13% and the average mass loss of WS at active pyrolysis zone is determined as about 45%. This case is another evidence of hemicellulose and cellulose decomposition occurs in the active pyrolysis zone.

TG and DTG curves of PP, LDPE, WS, WS/PP and WS/LDPE blends for the blending ratio of 1:1 are given in Figs. 4 and 5 (heating rate of 20 °C min^{-1}). According to the curves, WS is decomposed at a lower temperature than plastics. Polyolefinic polymers, like PP and LDPE have almost same trends, this is indicates that they have the same pyrolysis behaviors due to similar chemical bonds in their molecular structures. Polyolefinic polymers are decomposed by random chain scission which is a very typical mechanism for polymer decomposition. The process is a multistep radical chain reaction with all the general features of such reaction mechanisms: initiation, propaganation, branching, and termination steps [8,10]. The weight losses show that degradation of plastics occurs almost totally in one-step process.

PP samples starts to react at temperature as low as 392 °C while LDPE samples begin to decompose at a higher temperature of 432 °C. The weight loss of all samples increased with temperature increasing. Since the chemical bonds in plastic break more easily at higher temperature, increase of weight loss with temperature is expected [39,49].

Table 3 shows that the characteristic properties of active pyrolysis zone of WS, PP, LDPE and their blends such as starting temperature (T_i), ending temperature (T_f), the peak temperature (T_p) and total mass loss (%). As the heating rate is increased, Table 3 shows that there was a lateral shift with an increase in the rate as the heating rate was increased from 5 to 50 °C min^{-1}. The displacement of TG curves with heating rate has been described in the literature by different researchers [3,4].

There are many arguments to explain these displacements. Many authors consider that a change in the mechanism of the reaction can be produced when there is a change in the heating rate. In contrast inefficient heat transfer from furnace to sample may produce large differences between the temperature of the furnace and that of the sample, which obviously increase with heating rate.

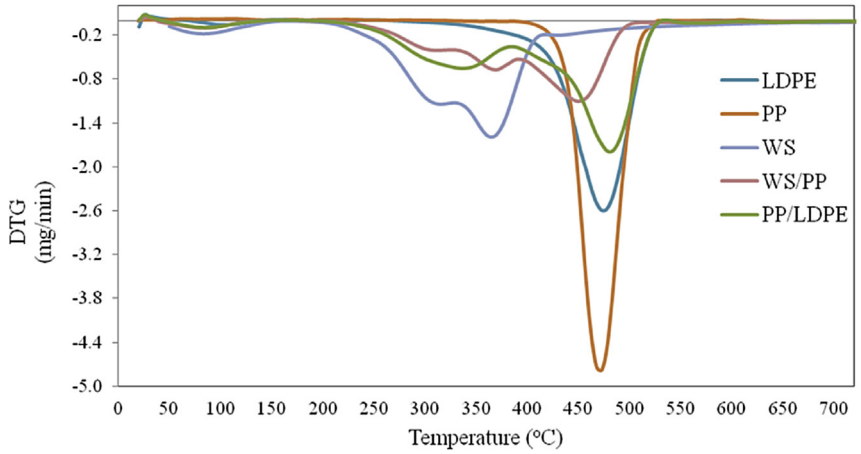

Fig. 5. DTG curves of LDPE, PP, WS, WS/PP and WS/LDPE.

Table 3
Properties of active pyrolysis zone at different heating rate.

	Heating rate (°C/min)	Pyrolysis range (°C)		Peak temperature (°C)	Total mass loss (%)
		T_i	T_f	T_p	
WS	5	208	365	348	68
	10	215	370	359	68
	15	230	410	360	69
	20	232	415	365	68
	50	248	440	379	56
PP	5	362	487	443	76
	10	366	492	457	75
	15	372	503	463	77
	20	392	511	473	76
	50	418	524	474	78
LDPE	5	385	501	459	74
	10	392	503	488	75
	15	413	514	484	73
	20	432	522	504	79
	50	443	544	509	76
WS:PP	5	189	460	290-345-415	64
1:1 mass ratio	10	188	479	300-359-435	64
	15	199	500	305-362-448	64
	20	199	500	310-369-450	64
	50	222	545	323-378-484	65
WS:LDPE	5	190	502	320–455	69
1:1 mass ratio	10	200	527	340–473	67
	15	203	531	342–475	65
	20	210	532	340–480	67
	50	213	564	428–504	67

TG curves of biomass and plastic sample blends lie between the ones of the individual samples. The characteristic temperatures for the blends change in comparison with those for each component. Co-components increase thermal stability of WS as can be concluded from the shift to T_{max} towards higher values.

To further illuminate whether interactions existed between the biomass and plastics, difference of weight loss ($\Delta w = w_{blend}-(x_1w_1+x_2w_2)$) is defined where w_{blend} is the weight loss of blend, x_i is the mass fraction of each material in the same operational conditions and w_i is the weight loss of each material in the same operational conditions. Δw describes the extent of synergistic effect which is calculated for different heating rate of 20 °C min^{-1} in Fig. 6 (For the blending ratio of 1:1). For WS-PP blends and WS-LDPE blends, co-components show a different behavior from that of individual samples. It can be seen that, for the two blends, Δw is less then ±5% before 390 °C because at this temperature PP and LDPE were still not decomposed, obviously there is no interaction between WS and plastic samples. A significant interaction is observed after about 392 °C for WS-PP blends which is the point of starting temperature of PP decomposition. These experimental results indicate a maximum synergistic effect during co-pyrolysis of WS-PP blends at 20 °C min^{-1} is about 16% at 448 °C. For WS-LDPE blends maximum synergistic effect during co-pyrolysis at 20 K min^{-1} is about −7% at 488 °C.

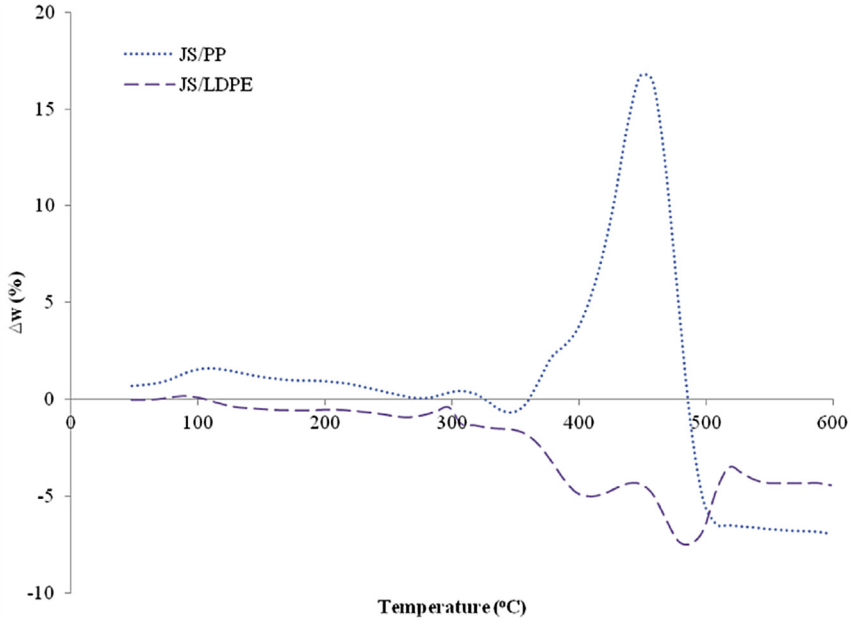

Fig. 6. Variation of Δw for WS-PP and WS-LDPE (1:1 mass ratio) blends (heating rate of 20 °C min^{-1}).

Table 4
Kinetic parameters for pyrolysis of WS, PP, LDPE and their blends from Arrhenius method.

Sample	Heating rate (°C min^{-1})		Activation energy (kJ mol^{-1})	Pre-exponential factor (min^{-1})	R^2
WS	5		69.11	1.87×10^{5}	0.976
	10		79.73	2.62×10^{6}	0.955
	15		61.00	4.91×10^{4}	0.984
	20		67.03	2.19×10^{5}	0.924
	50		69.71	6.48×10^{5}	0.982
PP	5		305.76	2.20×10^{21}	0.908
	10		298.74	2.04×10^{20}	0.943
	15		279.53	3.00×10^{19}	0.950
	20		295.11	3.51×10^{20}	0.960
	50		299.13	7.17×10^{20}	0.991
LDPE	5		256.58	3.82×10^{17}	0.973
	10		255.56	3.24×10^{17}	0.978
	15		247.86	1.01×10^{17}	0.987
	20		224.30	4.20×10^{15}	0.990
	50		288.45	4.54×10^{19}	0.984
WS/PP	5	1.stage	69.30	5.34×10^{4}	0.786
1:2 mass ratio	10	1.stage	57.60	5.92×10^{3}	0.882
	15	1.stage	59.51	9.37×10^{3}	0.910
	20	1.stage	67.62	4.07×10^{4}	0.898
	50	1.stage	71.23	4.59×10^{5}	0.901
WS/PP	5	1.stage	120.68	5.35×10^{10}	0.960
1:1 mass ratio		2.stage	169.79	1.32×10^{14}	0.972
		3.stage	103.66	1.42×10^{7}	0.987
	10	1.stage	112.21	1.06×10^{10}	0.960
		2.stage	134.29	7.25×10^{10}	0.982
		3.stage	116.57	1.60×10^{8}	0.997
	15	1.stage	108.89	5.20×10^{9}	0.978
		2.stage	152.30	3.22×10^{12}	0.987
		3.stage	109.63	5.01×10^{7}	0.992
	20	1.stage	113.24	1.64×10^{10}	0.989
		2.stage	141.06	3.42×10^{11}	0.986
		3.stage	122.00	4.77×10^{8}	0.997
	50	1.stage	105.46	3.42×10^{9}	0.980
		2.stage	117.94	4.09×10^{9}	0.945
		3.stage	193.23	2.59×10^{13}	0.893
WS/PP	5	1.stage	103.76	3.51×10^{7}	0.653
2:1 mass ratio		2.stage	264.51	1.22×10^{18}	0.872
	10	1.stage	86.71	7.09×10^{6}	0.796
		2.stage	268.15	5.55×10^{18}	0.990
	15	1.stage	74.66	7.81×10^{5}	0.986
		2.stage	211.03	4.31×10^{14}	0.991
	20	1.stage	75.12	1.13×10^{6}	0.980
		2.stage	142.47	4.00×10^{9}	0.840
	50	1.stage	79.24	7.22×10^{7}	0.905
		2.stage	158.45	1.89×10^{8}	0.891
WS/LDPE	5	1.stage	78.34	1.02×10^{6}	0.980
1:2 mass ratio		2.stage	256.71	3.18×10^{17}	0.979
	10	1.stage	74.99	6.87×10^{5}	0.986
		2.stage	256.14	3.04×10^{17}	0.990
	15	1.stage	79.14	1.84×10^{6}	0.956
		2.stage	184.85	4.11×10^{12}	0.981
	20	1.stage	76.79	1.42×10^{6}	0.965
		2.stage	188.77	9.52×10^{12}	0.972
	50	1.stage	81.49	2.54×10^{6}	0.908
		2.stage	204.48	8.95×10^{12}	0.899
WS/LDPE	5	1.stage	86.72	6.61×10^{6}	0.938
1:1 mass ratio		2.stage	156.58	3.01×10^{10}	0.991
	10	1.stage	86.41	9.79×10^{6}	0.962
		2.stage	146.99	8.74×10^{9}	0.989
	15	1.stage	97.17	1.06×10^{8}	0.951
		2.stage	162.59	1.47×10^{11}	0.946
	20	1.stage	84.61	9.91×10^{6}	0.978
		2.stage	152.84	3.56×10^{10}	0.951
	50	1.stage	75.35	1.99×10^{6}	0.978
		2.stage	197.75	3.21×10^{13}	0.909
WS/LDPE	5	1.stage	89.93	4.87×10^{6}	0.983
2:1 mass ratio		2.stage	133.18	8.62×10^{8}	0.976
	10	1.stage	85.43	8.94×10^{6}	0.952
		2.stage	149.66	2.03×10^{10}	0.972
	15	1.stage	86.81	1.52×10^{7}	0.977
		2.stage	144.73	1.03×10^{10}	0.959
	20	1.stage	89.84	3.11×10^{7}	0.980
		2.stage	141.33	6.0×10^{9}	0.962
	50	1.stage	91.45	2.58×10^{7}	0.981
		2.stage	151.35	8.01×10^{9}	0.915

3.2. Kinetic analysis

Non-isothermal kinetic study of carbonaceous materials is an extremely composite task because of the presence of numerous complex components and their parallel and consecutive reactions [45]. The decomposition rate during thermal treatment can be represented by the following equation:

$$\frac{dx}{dT} = kf(x)^n \tag{2}$$

where f(x) = (1−x), x is the extent of conversion, t is the time, k is the specific rate constant and n is the order of reaction. The extent of conversion can be represented as follows:

$$x = \frac{w_o - w_t}{w_o - w_f} \tag{3}$$

where w_o is the initial mass of the sample, w_t is the actual mass and w_f is the mass after pyrolysis. The reaction rate constant, k, is modeled by Arrhenius equation, whereby:

$$k(T) = Ae^{\frac{-E_a}{RT}} \tag{4}$$

R is the universal gas constant, E_a the activation energy and A the pre-exponential (or frequency) factor, a gauge of the collision frequency of molecules during a reaction related to the number of molecules present in a given volume [46]. For constant heating rate, β, a linear relation between time and temperature can be written as:

$$T = T_o + \beta t \tag{5}$$

Now, substituting Eqs. (4) and (5) in (2) and rearranging, the expression becomes:

$$\frac{dx}{dT} = \frac{A}{\beta} e^{-E_a/RT}(1-x)^n \tag{6}$$

The above equation can be used to evaluate E_a and A at constant heating rate using TG data. However, the right hand side of Eqn. (6) has no definite integral which makes it difficult to find the exact solution. Therefore, several methods were developed to estimate the value of E_a and A [41].

In Arrhenius method the final rate equation given below is obtained by linearization of Eq. (6) and making some rearrangements:

$$ln\left(\frac{dx}{dT}\right) - nln(1-x) = ln\left(\frac{A}{\beta}\right) - \frac{E_a}{RT} \tag{7}$$

The plot of ln(dx/dT)−nln(1−x) versus (1/T) should give a straight line for the correct value of reaction order n. The activation energy and pre-exponential factors are calculated from slope ($-E_a/R$) and interception (ln(A/β)), respectively [4].

In Coats Redfern method, an asymptotic approximation for the resolution of Eq. (6) gives,

$$ln\left[-\frac{ln(1-x)}{T^2}\right] = ln\left[\frac{AR}{\beta E_a}\right] - \frac{E_a}{RT} \quad (n=1) \tag{8}$$

Above Eq. (8) will result in a straight line with slope $-E_a/R$ and an intercept of ln [$AR/\beta E_a$]. This was done by plotting graph between following [14,32]:

$$ln\left[-\frac{ln(1-x)}{T^2}\right] \ versus \ 1/T \quad (n=1)$$

Kinetic parameters were calculated for the blending ratios of 1:2, 1:1 and 2:1 with the applied heating rates of 5, 10, 15, 20 and 50 K min^{-1}. For individual samples and their blends (1:2, 1:1 and 2:1 mass ratio) calculated activation energies and pre-exponential factors by using Arrhenius method and Coats Redfern method were given at Tables 4 and 5, respectively. Considering the results tabulated in Tables 4 and 5, it can be said that the kinetic parameter values were affected from the variations in heating rates. When comparing the results with those of the thermal decomposition of the single materials, it is noteworthy that the activation energies of polyolefin in the blends were lower than the activation energies of single polyolefin for applied heating rates. Also decreasing of the activation energies are due to the probable influence of products formed during WS degradation on polyolefin degradation. This behavior was also noted for blends of biomass derivatives with other common polymers with changes in the mechanism of thermal degradation [2,39].

The activation energy obtained from the Coats Redfern method for WS, PP, LDPE and their blends are mostly higher than that obtained from the Arrhenius method. Some researchers have studied out that activation energy values are influenced by the temperature interval of pyrolysis, method of mathematical analysis, pyrolysis techniques, and others. So the literature offers a wide range of values of activation energy [18]. The variation between Arrhenius and Coats Redfern methods encountered in this study can be generally attributed to the approximations of the method used for determination of kinetic parameters.

The results of calculated x values using the predicted kinetic parameters by the Arrhenius and Coats Redfern method have been compared to those experimental and are shown in Figs. 7 and 8 for the heating rate of 20 K min^{-1} and blending ratio 1:1. It can be seen from the figures, all the calculated curves almost overlap with the experimental ones. In general, experimental values of x are lower than the calculated values.

Table 5
Kinetic parameters for pyrolysis of WS, PP, LDPE and their blends from Coats-Redfern method.

Sample	Heating rate (°C min^{-1})		Activation energy (kJ mol^{-1})	Pre-exponential factor (min^{-1})	R^2
WS	5		102.31	2.74×10^5	0.962
	10		109.83	1.95×10^6	0.955
	15		97.51	1.07×10^5	0.963
	20		89.78	8.18×10^4	0.957
	50		108.45	1.66×10^8	0.982
PP	5		336.16	5.27×10^{23}	0.963
	10		315.81	1.59×10^{22}	0.971
	15		308.92	4.04×10^{21}	0.977
	20		314.32	9.58×10^{21}	0.982
	50		392.45	2.34×10^{27}	0.951
LDPE	5		309.17	2.36×10^{21}	0.985
	10		276.79	9.28×10^{18}	0.990
	15		286.89	5.12×10^{19}	0.992
	20		302.81	9.18×10^{20}	0.982
	50		408.19	6.22×10^{22}	0.906
WS/PP	5	1.stage	72,82	$9,60 \times 10^4$	0,930
1:2 mass ratio	10	1.stage	64.63	2.07×10^4	0.957
	15	1.stage	64.25	1.83×10^4	0.953
	20	1.stage	69.54	4.36×10^4	0.957
	50	1.stage	70.59	7.89×10^4	0.963
WS/PP	5	1.stage	51.02	5.07×10^3	0.887
1:1 mass ratio		2.stage	251.50	1.24×10^{21}	0.999
		3.stage	149.39	4.44×10^{10}	0.996
	10	1.stage	44.39	1.67×10^3	0.852
		2.stage	199.58	1.87×10^{16}	0.996
		3.stage	180.76	9.49×10^{12}	0.992
	15	1.stage	49.80	7.82×10^3	0.895
		2.stage	237.84	3.63×10^{19}	0.997
		3.stage	166.02	6.92×10^{11}	0.993
	20	1.stage	52.53	1.71×10^4	0.873
		2.stage	211.04	1.76×10^{17}	0.996
		3.stage	183.64	1.46×10^{13}	0.993
	50	1.stage	122.61	1.10×10^{11}	0.971
		2.stage	188.54	1.34×10^{15}	0.965
		3.stage	270.23	5.77×10^{18}	0.988
WS/PP	5	1.stage	101.86	2.67×10^7	0.918
2:1 mass ratio		2.stage	282.59	2.73×10^{19}	0.969
	10	1.stage	101.01	1.42×10^8	0.878
		2.stage	308.04	3.96×10^{21}	0.997
	15	1.stage	88.18	1.09×10^7	0.972
		2.stage	271.10	7.52×10^{18}	0.981
	20	1.stage	89.58	1.83×10^7	0.972
		2.stage	164.06	1.45×10^{11}	0.952
	50	1.stage	95.49	2.89×10^8	0.948
		2.stage	248.59	4.89×10^{18}	0.974
WS/LDPE	5	1.stage	94.11	2.41×10^7	0.963
1:2 mass ratio		2.stage	326.05	2.67×10^{22}	0.983
	10	1.stage	89.83	1.28×10^7	0.968
		2.stage	308.80	1.60×10^{21}	0.991
	15	1.stage	99.10	1.02×10^8	0.942
		2.stage	221.07	1.32×10^{15}	0.992
	20	1.stage	94.76	4.96×10^7	0.955
		2.stage	237.32	2.40×10^{16}	0.989
	50	1.stage	95.48	9.57×10^7	0.908
		2.stage	240.68	3.48×10^{16}	0.941
WS/LDPE	5	1.stage	70.30	1.74×10^5	0.992
1:1 mass ratio		2.stage	192.18	1.05×10^{13}	0.988
	10	1.stage	68.21	1.87×10^5	0.989
		2.stage	182.27	2.72×10^{12}	0.988
	15	1.stage	68.05	2.17×10^5	0.973
		2.stage	183.52	3.82×10^{12}	0.986
	20	1.stage	71.134	5.22×10^5	0.992
		2.stage	178.94	2.16×10^{12}	0.983
	50	1.stage	58.760	5.75×10^4	0.984
		2.stage	240.51	2.39×10^{16}	0.968
WS/LDPE	5	1.stage	100.51	1.55×10^8	0.965
2:1 mass ratio		2.stage	161.35	9.32×10^{10}	0.983
	10	1.stage	99.12	1.48×10^8	0.953
		2.stage	186.29	8.54×10^{12}	0.975
	15	1.stage	102.98	4.06×10^8	0.958
		2.stage	175.58	1.54×10^{12}	0.969
	20	1.stage	105.16	6.73×10^8	0.969
		2.stage	169.37	5.44×10^{11}	0.981
	50	1.stage	110.15	9.78×10^8	0.974
		2.stage	170.26	7.69×10^{10}	0.967

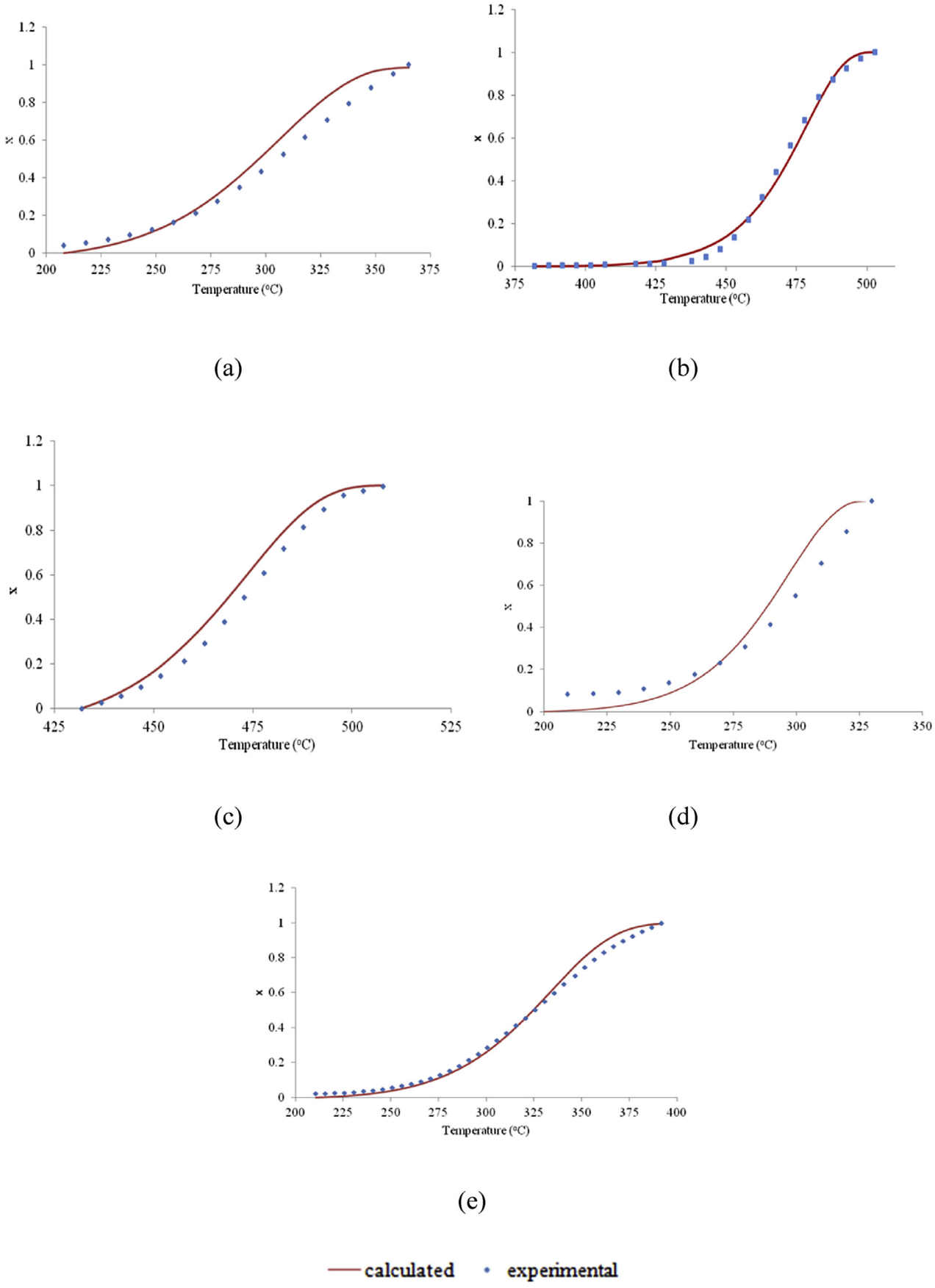

Fig. 7. Comparison of experimental and model values of x vs. temperature from Arrhenius Method (20 K min^{-1}, 1:1 mass ratio, 1.stage) a. WS, b. PP, c. LDPE, d. WS/PP, e. WS/LDPE.

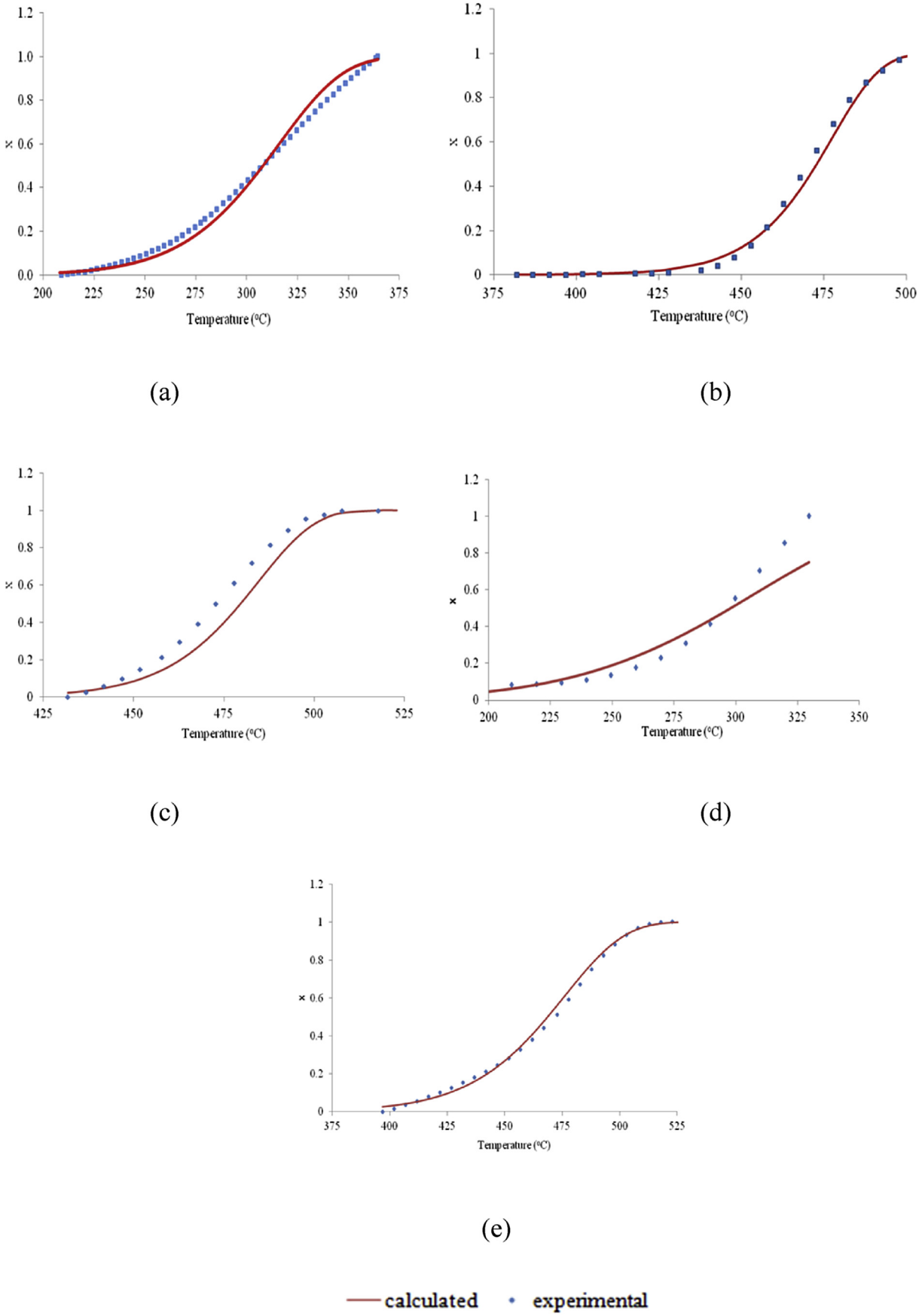

Fig. 8. Comparison of experimental and model values of x vs. temperature from Coats–Redfern Method (20 K min^{-1}, 1:1 mass ratio, 1.stage) a. WS, b. PP, c. LDPE, d. WS/PP, e. WS/LDPE.

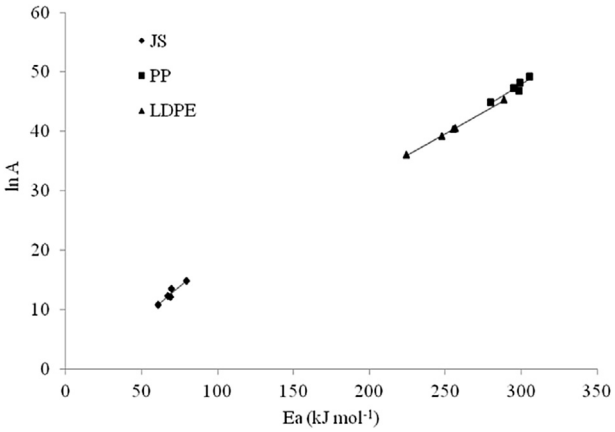

Fig. 9. The kinetic compensation effect analysis curves of WS, PP and LDPE.

3.3. Kinetic compensation effect

The kinetic compensation effect states that there is a linear relationship between Arrhenius parameters log(A) and E for a family of related processes. It is a widely observed phenomenon in many areas of science, notably heterogeneous catalysis [5,6,16]. The applicability of the Arrhenius equation to a particular reaction could be tested by finding constancy or a predictable variation in the "frequency factor" with changes in experimental conditions or sample treatment or structure. It is demonstrated, both theoretically and by numerically, that random errors in kinetic data do generate an apparent compensation effect (sometimes termed the statistical compensation effect) when the true Arrhenius parameters are constant [44,48].

Expressions for the gradient of data points on a plot of log(A) against E_a are derived when experimental kinetic data are analyzed by linear regression.

$$\ln A = \omega + \varepsilon E_a \tag{9}$$

where ω and ε are the coefficients of linear regression, which depend on the type of sample and their structures. Fig. 9 shows the kinetic compensation effect analysis curves of *WS*, PP and LDPE. The linear fitting of ln A and E_a is carried out based on the calculated kinetic parameters through Arrhenius method, and the relationship between ln A and E_a can be expressed as following:

$$\ln A = 0.2117\, E_a - 1.9919 \quad R^2 = 0.925 \quad (WS)$$

$$\ln A = 0.1551\, E_a + 1.3976 \quad R^2 = 0.904 \quad (PP)$$

$$\ln A = 0.14531\, E_a + 3.2586 \quad R^2 = 0.999 \quad (LDPE)$$

The validity of the compensation effect is not generally accepted and it is often considered as a statistical deviation (an artifact), due to the extrapolation necessary to calculate the A values. However, previous researchers proved the importance of the compensation phenomenon on the kinetic parameters A and E, and gave several correlations between them and theoretic interpretations for that phenomenon as well [20,35,43].

4. Conclusion

TG and DTG curves provide valuable information on pyrolysis mechanism and kinetics of biomass and plastic samples. This knowledge is very important for industrial scale application. For this purpose non-isothermal TG analyses of WS, PP, LDPE and their blends have been carried out in 50–650 °C temperature range at 5, 10, 15, 20 and 50 °C min^{-1} heating rates under nitrogen flow (20 mL min^{-1}). For WS pyrolysis, three distinct mass loss zones were determined which were attributed to removal of water, decomposition of hemicelluloses and cellulose and decomposition of lignin, respectively. In the second zone named as active pyrolysis zone most of the mass loss has occurred about 45%. Based on this result, walnut shell was found to have considerable potential for pyrolysis processes. It is found that the heating rate has a significant effect on the pyrolysis process. The weight loss region is shifted to a higher temperature range for all materials. The overall rate equations for various heating rate were determined by Arrhenius and Coats–Redfern equations. According to Arrhenius method, the average value of activation energies of WS, PP and LDPE were 69.32, 295.65 and 254.55 kJ mol^{-1}, respectively. Moreover by using Coats Redfern method, average value of activation energies of WS, PP and LDPE were determined as 101.58, 333.53 and 316.77 kJ mol^{-1}, respectively. Kinetic compensation effect was observed clearly for all samples which is useful for the designing of pyrolysis units.

Acknowledgments

The authors are grateful to 'Anadolu University Scientific Research Projects Council' for the financial support of this work through the project 1205F104.

References

[1] A. Aboulkas, K. El Harfi, A. El Bouadili, M. Ben Chana, A. Mokhlisse, Pyrolysis kinetics of polypropylene, J. Therm. Anal. Calorim. 89 (2007) 203–209.
[2] A. Aboulkas, K. El Harfi, A. El Bouadili, M. Nadifiyine, M. Benchanaa, A. Mokhlisse, Pyrolysis kinetics of olive residue/plastic mixtures by non-isothermal thermogravimetry, Fuel Process. Technol. 90 (2009) 722–728.
[3] A. Aboulkas, K. El Harfi, A. El Bouadili, Thermal degradation behaviours of polyethylene and polypropylene. Part I: pyrolysis kinetics and mechanisms, Energy Convers. Manag. 51 (2010) 1363–1369.
[4] K. Açıkalın, Thermogravimetric analysis of walnut shell as pyrolysis feedstock, J. Therm. Anal. Calorim. 105 (2011) 145–150.
[5] P.J. Barrie, The mathematical origins of the kinetic compensation effect: 1. The effect of random experimental errors, Phys. Chem. Chem. Phys. 14 (2012a) 318–326.
[6] P.J. Barrie, The mathematical origins of the kinetic compensation effect: 2. The effect of systematic errors, Phys. Chem. Chem. Phys. 14 (2012b) 327–336.
[7] S.H. Beis, O. Onay, E. Atabay, O.M. Kockar, Pyrolysis of Walnut Shell in a Fixed-bed Reactor, World Renewable Energy Congress VI, 2000, pp. 1360–1363 (WREC2000).
[8] C.L. Beyler, M.M. Hirschler, The SFPE Fire Protection Engineering, 2002 (chapter 7): 'Thermal decomposition of polymers'.
[9] N. Bilanzija, V. Jurisic, N. Voca, J. Leto, A. MAtin, S. Sito, T. Kricka, Combustion properties of Miscanthus x giganteus biomass e Optimization of harvest time, J. Energy Inst. 90 (4) (2017) 528–533.
[10] H. Bockhorn, A. Hornung, U. Hornung, D. Schawaller, Kinetic study on the thermal degradation of polypropylene and polyethylene, J. Anal. Appl. Pyrolysis 48 (1999) 93–109.
[11] M. Brebu, S. Ucar, C. Vasile, J. Yanik, Co-pyrolysis of pine cone with synthetic polymers, Fuel 89 (2010) 1911–1918.
[12] C.R. Cardoso, M.R. Miranda, K.G. Santos, C.H. Ataide, Determination of kinetic parameters and analytical pyrolysis of tobacco waste and sorghum bagasse, J. Anal. Appl. Pyrolysis 92 (2011) 392–400.
[13] J. Ceamanos, J.F. Mastral, A. Millera, M.E. Aldea, Kinetics of pyrolysis of high density polyethylene. Comparison of isothermal and dynamic experiments, J. Anal. Appl. Pyrolysis 65 (2) (2002) 93–110.
[14] A.W. Coats, J.P. Redfern, Kinetic parameters from thermogravimetric data, Nature 201 (1964) 68–69.
[15] A. Demirbas, Effect of temperature on pyrolysis products from four nut shells, J. Anal. Appl. Pyrolysis 76 (2006) 285–289.
[16] D. Dollimore, P.F. Rodgers, The appearance of a compensation effect in the thermal decomposition of manganese (II) carbonates, prepared in presence of other metal ions, Thermochim. Acta 30 (1979) 273–280.
[17] R. Ebrahimi-Kahrizsangi, Evaluation of reliability of Coats-Redfern method for kinetic analysis of non-isothermal TGA, Trans. Nonferrous Metals Soc. China 18 (1) (2008) 217–221.
[18] S.A. El-Sayed, M.E. Mostafa, Pyrolysis characteristics and kinetic parameters determination of biomass fuel powders by differential thermal gravimetric analysis (TGA/DTG), Energy Conv. Manag. 85 (2014) 165–172.
[19] L.M.T. Frija, C.A.M. Afonso, Supported acid-catalyzed flash vacuum thermolysis on the valorisation of labdanum resin, Biomass Bioenergy 71 (2014) 363–369.
[20] A.K. Galwey, Compensation parameters in heterogenous catalysis, J. Catal. 60 (1979) 335–338.
[21] A.E. Ghaly, K.G. Mansaray, Comparative study on the thermal degradation of Rice Husk in Various atmospheres, Energy Sources 21 (1999) 867–881.
[22] J.H. Harker, J.R. Backhurst, Fuel and Energy, Academic Press Limited, London, 1981.
[23] Y. Kar, Co-pyrolysis of walnut shell and tar sand in a fixed-bed reactor, Bioresour. Technol. 102 (2011) 9800–9805.
[24] T. Kolb, M. Aigner, R. Kneer, M. Müller, R. Weber, N. Djordjevic, Tackling the challenges in modelling entrained-flow gasification of low-grade feedstock, J. Energy Inst. 89 (4) (2016) 485–503.
[25] S. Li, S. Xu, S. Liu, C. Yang, Q. ve Lu, Fast pyrolysis of biomass in free-fall reactor for hydrogen-rich gas, Fuel Process. Tech. 85 (2004) 1201–1211.
[26] M.A. Lopez-Velazquez, V. Santes, J. Balmaseda, E. Torres-Garcia, Pyrolysis of orange waste: a thermo-kinetic study, J. Anal. App. Pyrolysis 99 (2013) 170–177.
[27] I. Martín-Gullón, M. Esperanza, R. Font, Kinetic model for the pyrolysis and combustion of poly-(ethylene terephthalate) (PET), J. Anal. Appl. Pyrolysis 58–59 (2001) 635–650.
[28] Y. Niu, F. Han, Y. Chen, Y. Lyu, L. Wang, Experimental study on steam gasification of pine particles for hydrogen-rich gas, J. Energy Inst. 90 (5) (2017) 715–724.
[29] A. Pattiya, S. Suttibak, Fast pyrolysis of sugarcane residues in a fluidised bed reactor with a hot vapour filter, J. Energy Inst. 90 (1) (2017) 110–119.
[30] D. Pradhan, Recovery of Value Added Fuels From Waste Polyolefins/Bicycle Tyre and Tube, Master of Technology (Research) in Chemical Engineering, National Institute of Technology, Rourkela, 2011.
[31] Y.C. Rotliwala, P.A. Parikh, Thermal degradation of rice-bran with high density polyethylene: a kinetik study, Korean J. Chem. Eng. 28 (3) (2011) 788–792.
[32] H.H. Sait, A. Hussain, A.A. Salema, F.N. Ani, Pyrolysis and combustion kinetics of date palm biomass using thermogravimetric analysis, Biosource Technol. 118 (2012) 382–389.
[33] D.K. Seo, S.S. Park, J. Hwang, T.U. Yu, Study of the pyrolysis of biomass using thermo-gravimetric analysis (TGA) and concentration measurements of the evolved, J. Anal. Appl. 89 (2010) 66–73.
[34] H. Shui, X. Ma, L. Yang, T. Shui, C. Pan, Z. Wang, Z. Lei, S. Ren, S. Kang, C.C. Xu, Thermolysis of biomass-related model compounds and its promotion on the thermal dissolution of coal, J. Energy Inst. 90 (3) (2017) 418–423.
[35] G. Skodras, G. Nenes, N. Zafeiriou, Low rank coal- CO_2 gasification: experimental study, analysis of the kinetic parameters by Weibull distribution and compensation effect, Appl. Therm. Eng. (2013) xxx, 1–8.
[36] K. Slopiecka, P. Bartocci, F. Fantozzi, Thermogravimetric analysis and kinetic study of poplar wood pyrolysis, Appl. Energy 97 (2012) 491–497.
[37] K. Sornek, M. Filipowicz, K. Rzepka, Study of clean combustion of wood in a stove-fireplace with accumulation, J. Energy Inst. 90 (4) (2017) 613–623.
[38] B.B. Uzun, Pyrolysis of Pirina and the Characterisation of Pyrolysis Products, Anadolu University, Institue of Applied Science, 2005 (PhD. thesis).
[39] B.B. Uzun, E. Yaman, Thermogravimetric characteristics and kinetics of scrap tyre and Walnut shell co-pyrolysis, Waste Manag. Res. 32 (10) (2014) 961–970.
[40] D. Vamvuka, M. Trikouvertis, D. Pentari, G. Alevizo, A. Stratakis, Characterization and evaluation of fly and bottom ashes from combustion of residues from vineyards and processing industry, J. Energy Inst. 90 (4) (2017) 574–587.
[41] V. Volli, M.K. Purkait, Physico-chemical properties and thermal degradation studies of commercial oils in nitrigen atmosphere, Fuel 117 (2014) 1010–1019.
[42] Q.M.K. Waheed, C. Wu, P.T. Williams, Pyrolysis/reforming of rice husks with a Niedolomite catalyst: influence of process conditions on syngas and hydrogen yield, J. Energy Inst. 89 (4) (2016) 657–667.
[43] M.C. Wilson, A.K. Galwey, Compensation effect in heterogeneous catalytic reactions including hydrocarbon formation on clays, Nature 243 (1973) 402–404.
[44] Q.L. Yan, M. Künzel, S. Zeman, R. Svoboda, M. Bartoskova, The effect of molecular structure on thermal stability, decomposition kinetics and reaction models of nitric esters, Thermochim. Acta 566 (2013) 137–148.
[45] Q. Yang, S. Wu, R. Lou, G. Lv, Analysis of wheat straw lignin by thermogravimetry and pyrolysis-gas chromatography/mass spectrometry, J. Anal. Appl. Pyrolysis 87 (2010) 65–69.
[46] P. Yangali, A.M. Celaya, J.L. Goldfarb, Co-pyrolysis reaction rates and activation energies of West Virginia coal and cherry pit blends, J. Anal. Appl. Pyrolysis 108 (2014) 203–211.
[47] Y. Zhang, D. Fan, Y. Zheng, Comparative study on combined co-pyrolysis/gasification of walnut shell and bituminous coal by conventional and congruent-mass thermogravimetric analysis (TGA) methods, Bioresour. Technol. 199 (2016) 382–385.
[48] C. Zou, l. Zhang, S. Cao, C. Zheng, A study of combustion characteristics of pulverized coal in O_2/H_2O atmosphere, Fuel 115 (2014) 312–320.
[49] L. Zhou, Y. Wang, Q. Huang, J. Cai, Thermogravimetric characteristics and kinetics of plastic and biomass blends co-pyrolysis, Fuel Process. Technol. 87 (2006) 963–969.
[50] B.B. Uzun, N. Sarioğlu, Rapid and catalytic pyrolysis of corn stalks, Fuel Process. Technol. 90 (2009) 705–716.
[51] TurkStat (Turkish Statistical Institute) 2014 Available at http://www.tuik. gov.tr/PreTablo.do?alt_id=1001.